

Microstructure and Phase Analysis of 3D Printed Components using Bronze Metal Filament

Zhe Lu^{1*}, Oyedotun Isaac Ayeni², Xuehui Yang², Hye-Yeong Park³, Yeon-Gil Jung³, Jing
Zhang^{1,**}

1. School of Materials and Metallurgical Engineering, University of Science and Technology of
Liaoning, China

2. Department of Mechanical and Energy Engineering, Indiana University - Purdue University
Indianapolis, USA

3. School of Materials Science and Engineering, Changwon National University, Republic of
Korea

Corresponding author: * lz19870522@126.com, **jz29@iupui.edu

Abstract

Typical metal 3D printing processes with powders require either a laser or electron beam as the heating source. In this work, an alternative non-expensive metal 3D printing process based on the fused deposition modeling (FDM) process using metal filled filament is studied. Using bronze filament as a feedstock, the microstructures, phases, compositions of the filament, as-printed, and sintered specimens are analyzed. The 3D printing process basically does not modify the morphology and phases of the filament. Sintering temperature below 832 °C is recommended. Above 832 °C, there are substantial oxidation reactions leading to the formation of copper oxide and cassiterite shell structure around the bronze core. The mechanical properties of the 3D printed sample are measured using the three-point bending test. The measured flexural strength is

This is the author's manuscript of the article published in final edited form as:

Lu, Z., Ayeni, O. I., Yang, X., Park, H.-Y., Jung, Y.-G., & Zhang, J. (2020). Microstructure and Phase Analysis of 3D-Printed Components Using Bronze Metal Filament. *Journal of Materials Engineering and Performance*, 29(3), 1650–1656.
<https://doi.org/10.1007/s11665-020-04697-x>

27.9 MPa, and the modulus of elasticity is 1.2 GPa. This study provides important information for applying the bronze filament in future engineering applications.

Keywords: metal filament; bronze; 3D printing; additive manufacturing; fused deposition modeling.

1. Introduction

Recently metal filled filaments used in the fused deposition modeling (FDM) process have been developed [1, 2]. In this metal filled filament method, polylactic acid (PLA) filaments contain a very fine metal powder, such as copper, bronze, brass, and stainless steel. The major advantage of this process is that it provides an alternative means to produce metallic components without using a laser or electron beam for typical metal powder bed fusion processes. The filaments can be printed using low cost FDM 3D printers. Additionally, the printed parts have a natural metallic finish which is aesthetically appealing. However, there are also some disadvantages: (1) Printed parts are very brittle; and (2) Metal filled filaments also tend to be very abrasive as they are extruded through the hot end. A standard brass nozzle will be relatively fragile and will quickly wear down. Therefore, it is recommended to upgrade to a wear resistant nozzle in order to print the filaments effectively.

Although there are some studies on their printability[3], the detailed study of their microstructure, phases, and mechanical properties for the as-printed and sintered components are still missing, which hinders future use of this economical metal 3D printing technique for engineering applications. Therefore, in this work, the FDM 3D printing process of bronze metal filament is studied. The work includes 3D printing and sintering at selected conditions. The

microstructure, phases, and mechanical property characterizations are carried out to provide better understanding of this relatively new process.

2. Experimental details

2.1. Bronze filament

The bronze filament (The Virtual Foundry, LLC, Stoughton, Wisconsin) used in this study contains at least 87% bronze metal and less than 13% PLA. A MakerBot Replicator 2 Desktop 3D Printer was used to print the specimens. The chemical properties of bronze filament are as follows [4]: melting temperature range $\sim 150 - 170$ °C; and thermal decomposition temperature greater than 240 °C.

2.2. 3D printing and sintering

In this work, the 3D printing method of FDM was used to print all the specimens. First, the CAD model was uploaded to the MakerBot software, which slices the CAD model and displays the estimated printing time and material use. The bronze filament was loaded to the printer to print. Once the print command was executed, the printer attained its target temperature which was set to 215 °C. The printing bed was moved to the home position, and the printer started to extrude the bronze filament from the nozzle. The melted filament was deposited to the printer bed layer by layer with a set layer height of 0.25 mm. After a layer was deposited, the printing platform descended by 0.25 mm and then continued to deposit the next layer.

After the 3D printed specimens were obtained, and then the specimens were sintered using a box furnace (Thermo Scientific Thermolyne Furnace, model FB1315M) to sinter the 3D printed specimens at three different temperatures of 150, 750, and 832 °C. 832 °C is the recommended

temperature by the filament manufacturer [4]. The other two lower temperatures were selected to evaluate the possible better sintering conditions.

2.3. Phase and microstructure analyses

Phase analysis for the prepared specimens was conducted using X-ray Diffractometer (Rigaku Miniflex II, Tokyo, Japan) with 0.02 °/step at the rate of 147.4 s/step. Microstructures of the specimens were investigated using a scanning electron microscope (SEM) with energy dispersive X-ray spectroscopy (EDS) (JEOL Model JSM-5610, Tokyo, Japan).

2.4. Three-point bending test

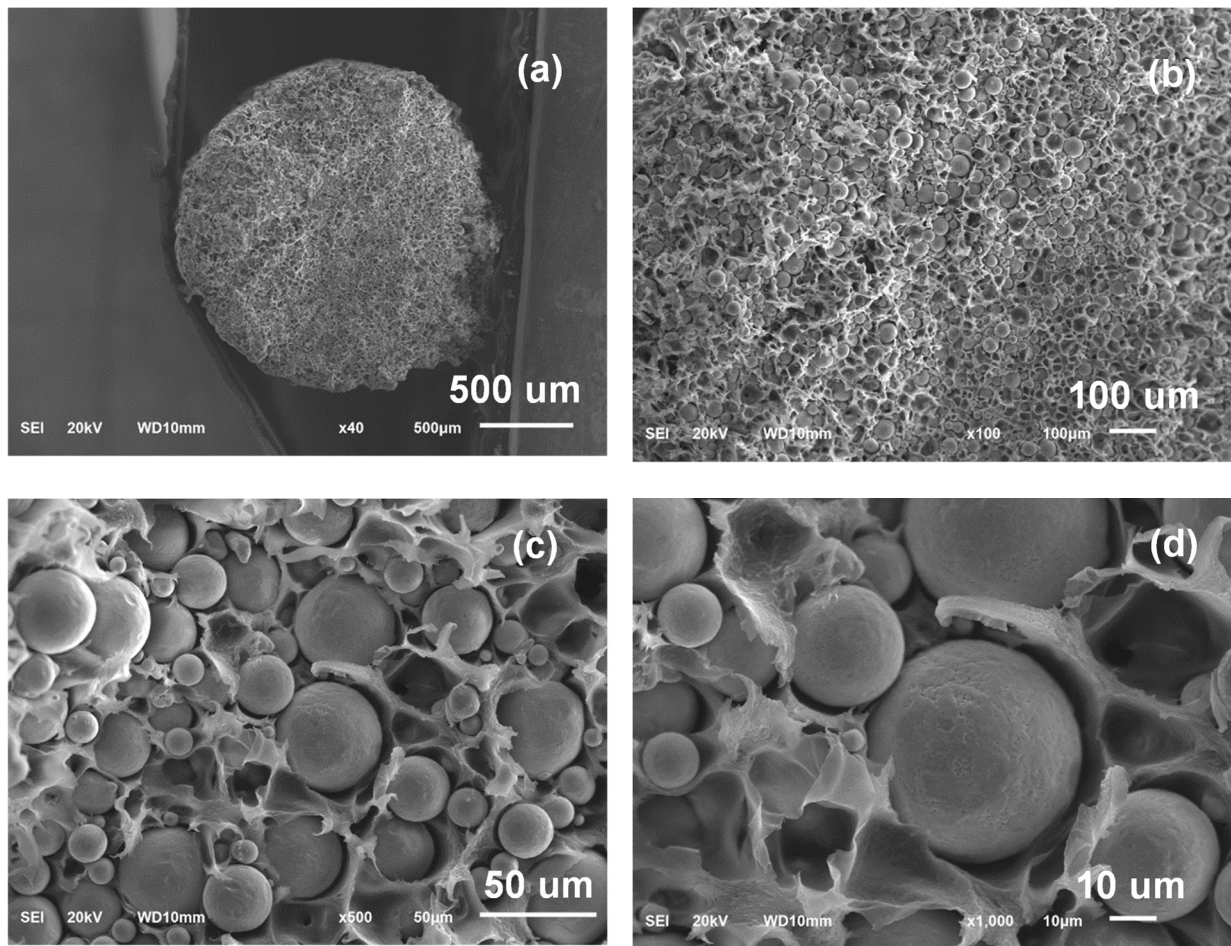
In order to characterize the mechanical properties of the printed components, the printed bar was subjected to three-point bending test to evaluate its mechanical strength, following the ASTM D790 [5].

3. Results and discussion

3.1. Bronze filament

The SEM images and EDS data of the bronze filament are given in Fig. 1. Fig. 1a shows the cross-sectional view of the filament. Fig. 1b shows that there is a large amount of bronze particles embedded in the PLA binder matrix. The high magnification images in Figs. 1c and 1d illustrate that the bronze particles are uniformly distributed inside the PLA binder matrix. The surface of the bronze particles is very smooth. The particle size of the bronze powder has a very broad distribution with an average size between 10~40 μm .

Fig. 1e shows the EDS result of the bronze powder and binder. The bronze powder contains (at. %) more Cu (46.78) and Sn (2.32), and fewer C (47.55) and O (3.35), while the polymer binder contains more C (85.55) and O (11.16), and fewer Cu (3.14) and Sn (0.15).



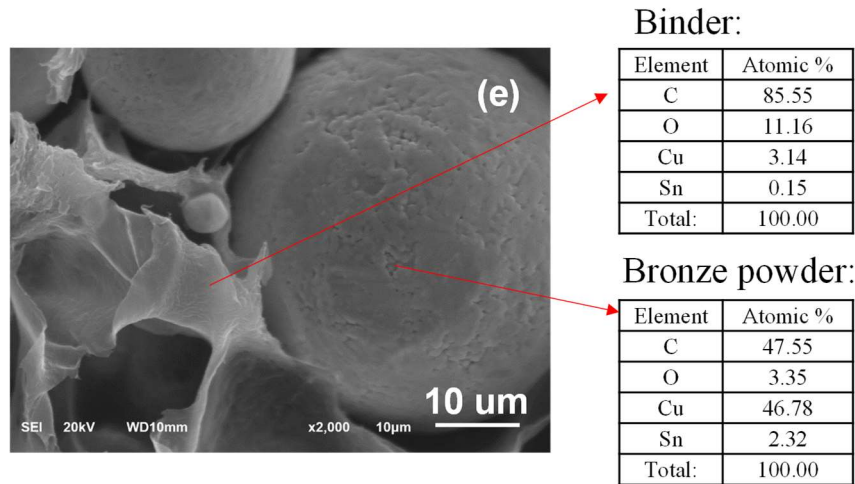


Figure 1: Microstructures of the bronze filament with different magnifications (a) $\times 40$, (b) $\times 100$, (c) $\times 500$, (d) $\times 1000$, and (e) $\times 2000$. The EDS results of the element analysis for the binder and bronze particle in the filament are also shown in (e).

3.2. 3D printed specimens

The SEM and EDS results of the 3D printed specimen are shown in Fig. 2. As shown in Fig. 2a, some of the filaments were compressed due to the heating in the 3D printing process. From Figs. 2b and 2c, the microstructures of 3D printed specimens are similar to those of the bronze filament shown in Fig 1. The binder in the outer layer of the filament experienced partial melting and solidification since the temperature of 3D printing process was 215 °C which exceeded the melting temperature of PLA. Fig. 2c also shows the EDS result which is basically same as that of the bronze filament with less than approximately 10% of difference, suggesting that the 3D printing process has little influence on the microstructure of the filament.

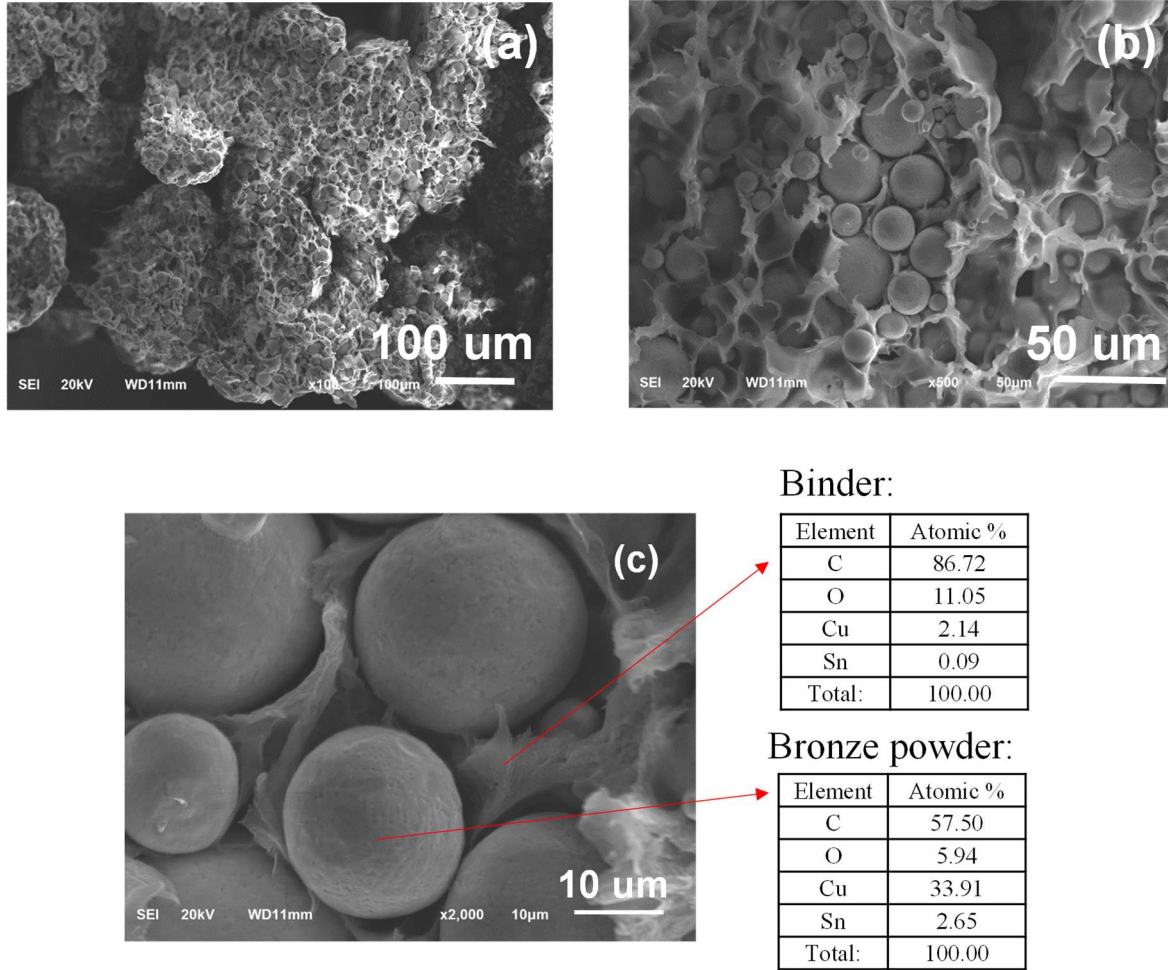


Figure 2: Microstructures of the as-printed specimens are shown in SEM images with different magnifications (a) $\times 100$, (b) $\times 500$, and (c) $\times 2000$. The EDS results of element analysis for the binder and bronze particle in the 3D printed specimen are also shown in (c).

3.3. Sintering of 3D printed specimens

The printed specimens were sintered at three different temperatures of 150, 750, and 832 °C, respectively. Figure 3 shows the SEM and EDS results of 3D printed specimen sintered at 150 °C. As is shown in Fig.3a, the macrostructure of the 3D printed specimen didn't change after annealing at 150°C. The surface of bronze particle became rough in the microstructure SEM

images. The EDS result shows the element components are almost same as the unannealed specimens, which means the temperature 150°C could melt partial binder part and make the boundary become fuzzy, but it could not change the distribution of the elements.

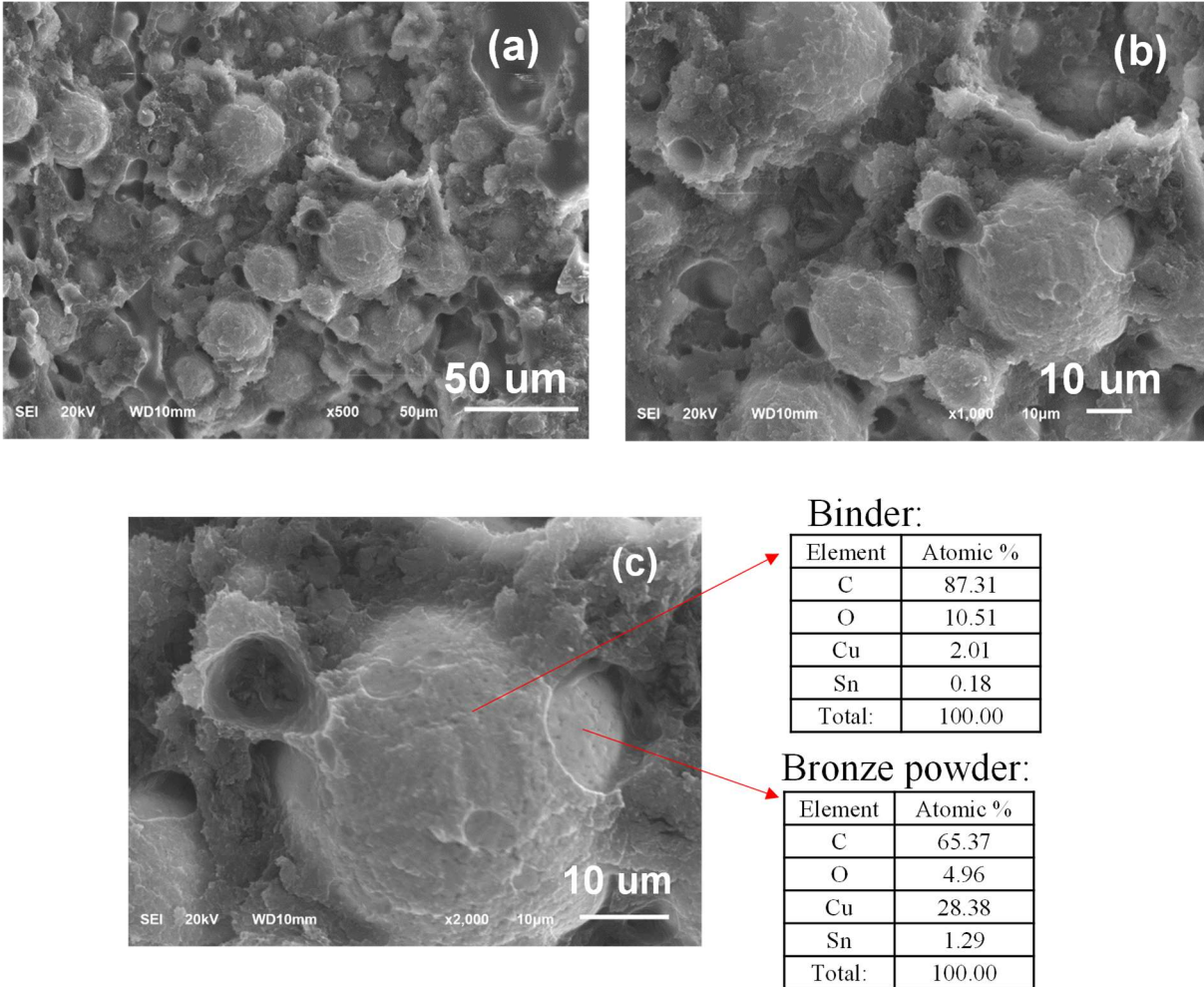


Figure 3: Microstructures of the sintered specimen at 150 °C at different magnifications. (a) ×500, (b) ×1000, and (c) ×2000. The EDS results of element analysis for the binder and bronze particle in the sintered specimen are also shown in (c).

Fig. 4 shows the SEM and EDS results of 3D printed specimen sintered at 750 °C. From Figs. 4a and 4b, the bronze particles show a rough surface. Some small white particles appeared on the surface, which may be caused by the oxidation reaction. Most binder were evaporated. The EDS data in Fig. 4c shows the ratio of Cu and Sn increased in the binder.

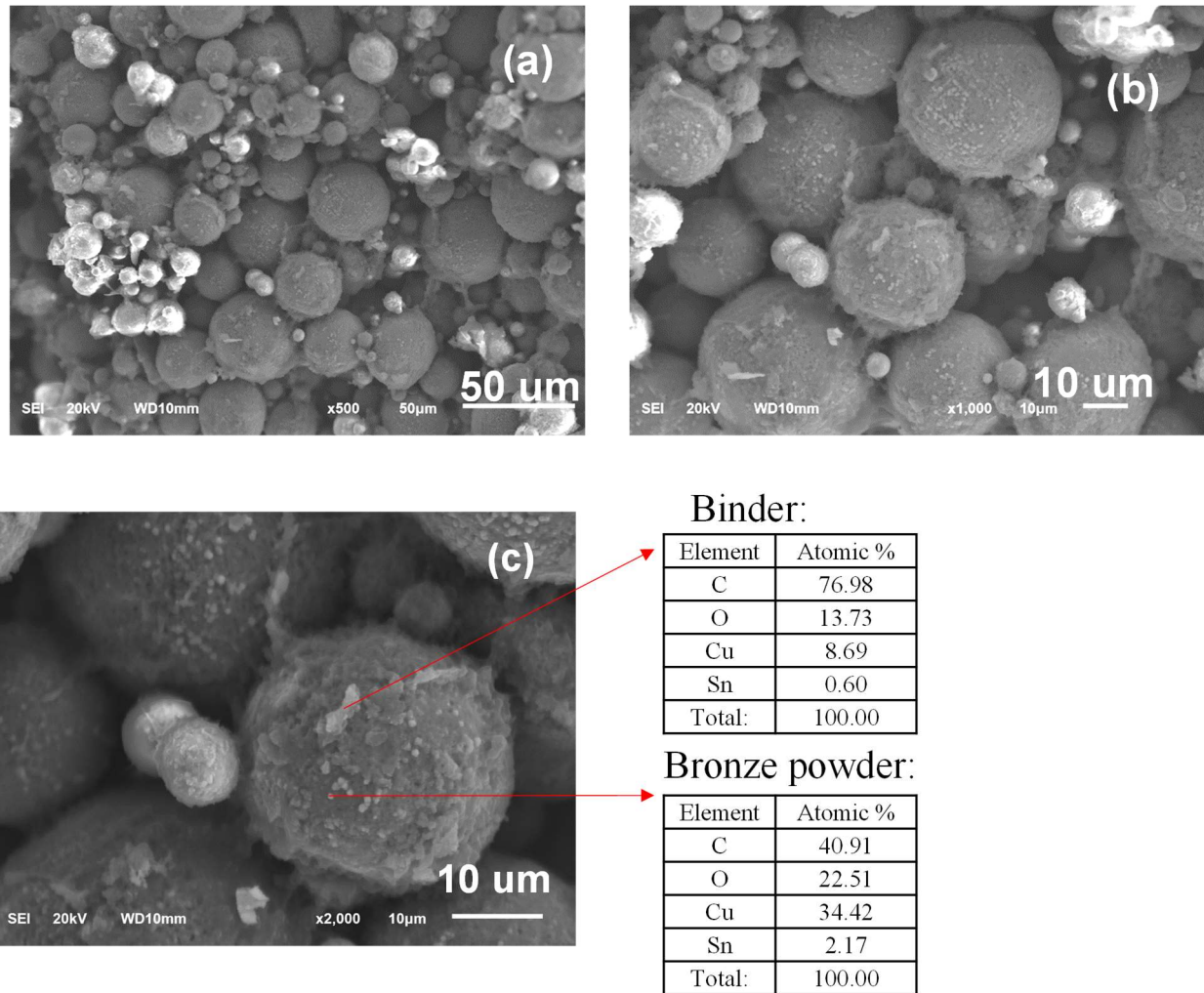
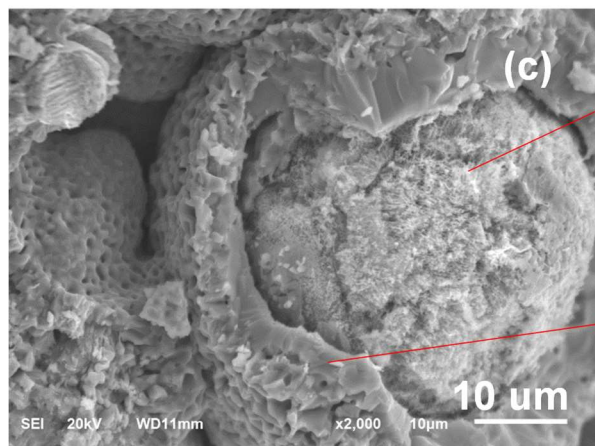
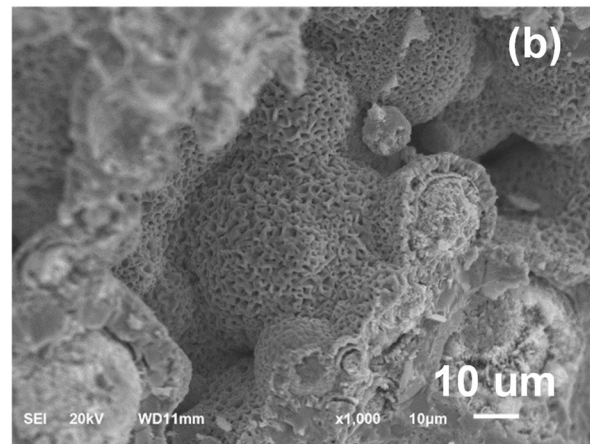
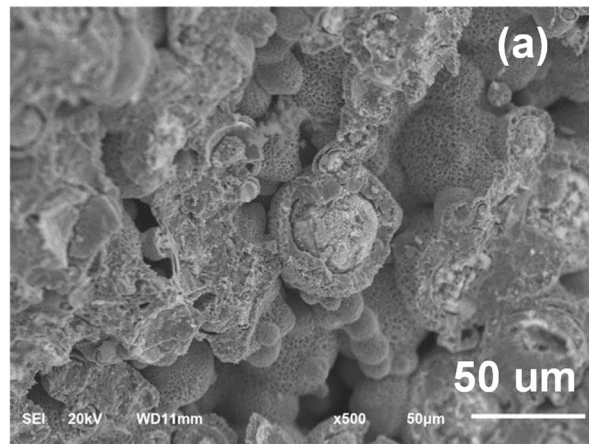


Figure 4: Microstructures of the sintered specimen at 750 °C with different magnifications. (a) $\times 500$, (b) $\times 1000$, and (c) $\times 2000$. The EDS results of element analysis for the binder and bronze particle in the sintered specimen are also shown in (c).

Figure 5 shows the SEM and EDS results of the 3D printed specimen sintered at 832 °C. The microstructure is totally different from the 3D printed specimens in Fig. 2 and low temperature cases in Figs. 3 and 4. First, the bronze particles showed porous surface, with a pore size about 1 μm . Secondly, there were extensive fractured particles with a core-shell structure. From the EDS data in Fig. 5c, the particle core are bronze and the outside shells are CuO, which is caused by the oxidization of Cu at high temperatures. The SEM image also shows that the blinder was completely evaporated at high temperatures.



Bronze powder core:

Element	Atomic %
C	26.66
O	48.70
Cu	23.63
Sn	1.01
Total:	100.00

Bronze powder shell:

Element	Atomic %
C	17.91
O	56.32
Cu	8.58
Sn	17.20
Total:	100.00

Figure 5: Microstructures of the sintered specimen at 832 °C with different magnifications. (a) $\times 500$, (b) $\times 1000$, and (c) $\times 2000$. The EDS results of element analysis for the binder and bronze particle in the sintered specimen are also shown in (c).

To understand the exact phase formed in the bronze filament and printed specimens, the XRD patterns of the bronze filament, as 3D printed specimen and 3D printed specimens at different sintering temperatures are summarized in Fig. 6. For the bronze filament, there are diffraction peaks at the 2θ of 42.2° , 49.1° , 72.3° and 87.5° , which are the peaks of copper-tin alloy. By comparing with the XRD pattern of as-printed specimen, the locations of the diffraction peaks are similar with the bronze filament, indicating that the process of 3D printing has little influence on changing the crystalline structure. The XRD patterns of the sintered specimens at 150°C and 750°C are basically same as that of the as-printed one, suggesting low sintering temperatures do not change the phase and microstructure of the as-printed specimen.

However, the XRD pattern of the 3D printed specimen sintered at 832°C is different from all the other cases. There are additional peaks except the peaks of copper-tin alloy of 42.2° and 72.3° . The peaks at 26.6° , 33.8° , 38.7° , 51.8° , 58.3° , and 66.1° are the characteristic peak of cassiterite, and the peaks at 32.4° , 35.6° , 36.5° , 48.9° , 61.5° , and 68.3° are copper oxide, as also observed in the EDS data and the shell structure in Fig. 5. Additionally, the intensity of the peaks of copper tin alloy is obviously lower than that of 3D printed specimens. Therefore, the heat treatment process at 832°C changed some copper-tin into cassiterite and copper oxide. Although 832°C is the recommended temperature by the filament manufacturer, it is clear that it is not an optimized temperature for the specimens in this study.

Moreover, based on the phase diagram of bronze, or 87% Cu and 13% Sn [6], when the sintering temperatures are between 150°C and 750°C, the phase of bronze is always the α phase. But when the sintering temperature reaches over 798°C, the β phase will occur, which is consistent with the different characteristic peaks of in the XRD patterns in Fig. 6.

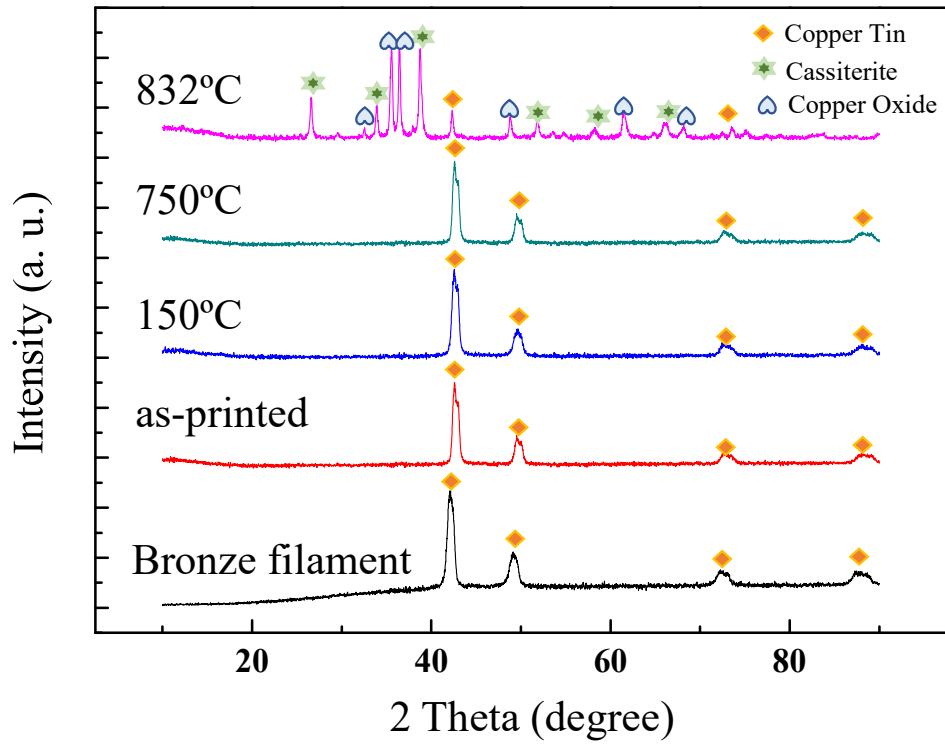


Figure 6: XRD patterns of the bronze filament, as-printed specimen, and sintered specimens at different temperatures.

3.4. Three-point bending of the printed specimen

For the three-point bending test, the specimen shows a typical stress versus strain curve as illustrated in Fig. 7. The curve has a nonlinear elastic deformation region, similar to many

plastics. From the curve, the derived flexural strength is 27.9 MPa, and the modulus of elasticity is 1.2 GPa.

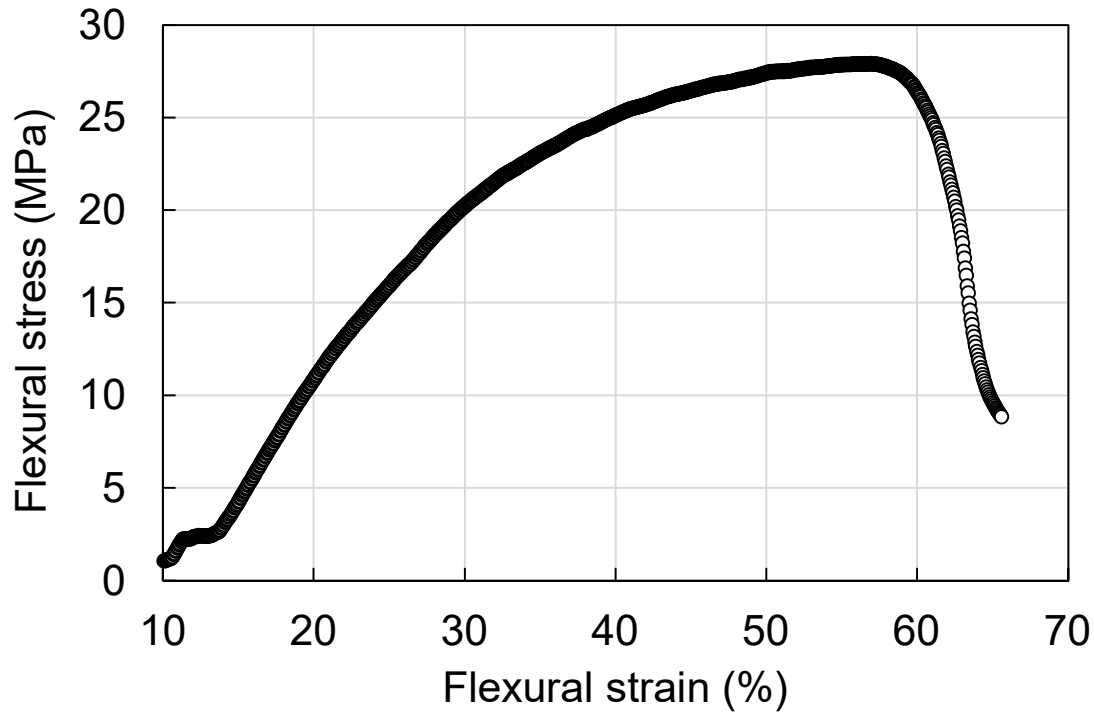


Figure 7: Flexural stress vs. strain curve in the three-point bending test.

The SEM fractography of the broken specimen is shown in Fig. 8. As shown in the figure, the fracture is primarily brittle in nature, compared to a typical ductile PLA filament. The presence of bronze particles reduces the flexibility of molecules chains' motion in the sample, causing a brittle fracture surface. Additionally, the bronze particles may act as a stress concentrator. These particles act as barriers to the propagation of microfractures produced in the PLA matrix during the plastic deformation of the sample. As the cracks are not able to progress when they reach a particle, the effective ductility is reduced [7].

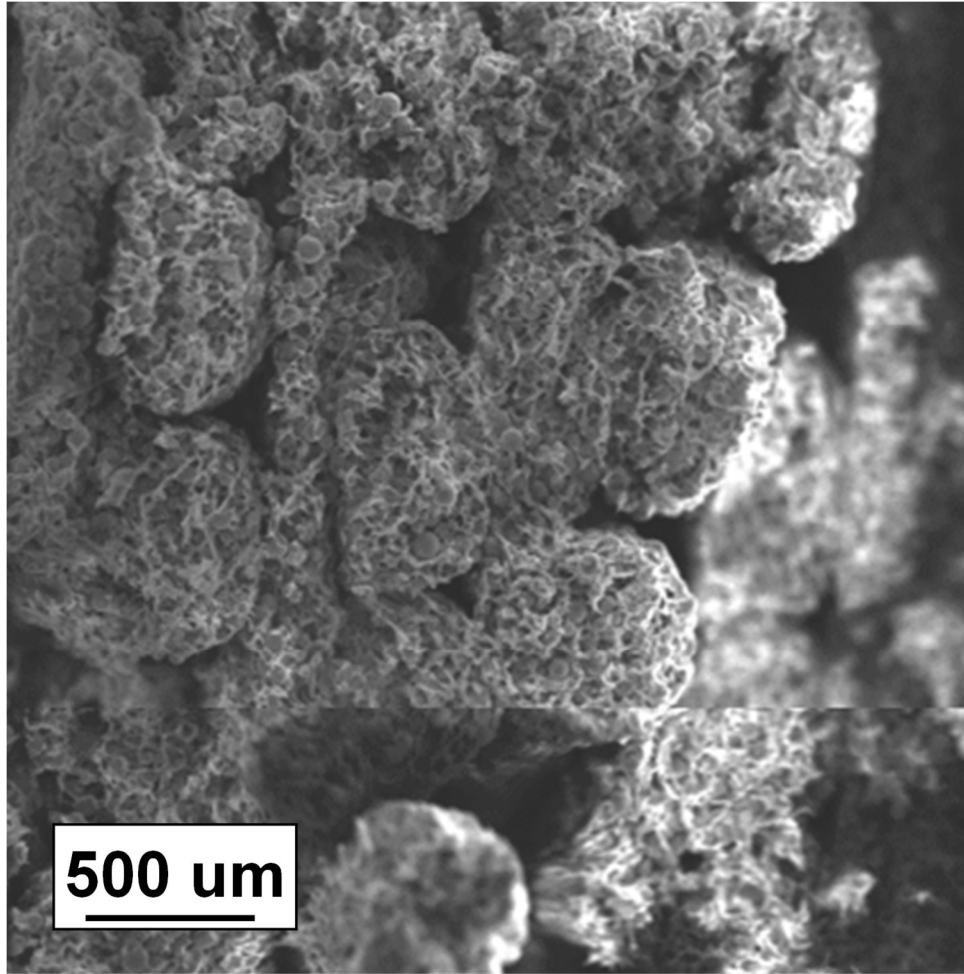


Figure 8: Fracture surface of the broken specimen.

4. Conclusions

In this study, the microstructures and phases of 3D printed bronze filaments have been studied.

The major results are summarized below:

1. 3D printing process basically does not modify the morphology and phases of the filament.
2. Sintering temperature below 832 °C is recommended. Above 832 °C, there are substantial oxidation reactions leading to the formation of copper oxide and cassiterite shell structure around the bronze core.

3. In the bronze filament, the spherical bronze particles are distributed in the PLA binder. The particle size of the bronze powder has a very broad distribution with the size size between 10~40 μm .
4. The mechanical properties were measured using the three-point bending test. The derived flexural strength is 27.9 MPa, and the modulus of elasticity is 1.2 GPa.
5. Brittle fracture is observed in the fracture surface in samples subjected to three-point bending test. This is due to the presence of bronze particles which reduces the flexibility of molecules chains' motion in the sample, causing a brittle fracture surface.

Acknowledgements

This work is partially supported by “Human Resources Program in Energy Technology (No. 20194030202450)”, “Power Generation & Electricity Delivery grant (No. 20181110100310)” of the Korea Institute of Energy Technology Evaluation and Planning (KETEP), and the National Natural Science Foundation of China (No. 51702145).

References

- [1] N. Hall. (2018) New filament means you can print metal on any 3D printer. *3D Printing Industry* (<https://3dprintingindustry.com/news/now-can-print-metal-3d-printer-85255/>, accessed October 20, 2019).
- [2] O. I. Ayeni, "Sintering and Characterizations of 3D Printed Bronze Metal Filament," M.S. thesis, Purdue University, 2018.
- [3] VirtualFoundry. (2018). *Bronze Filamet* (<https://www.thevirtualfoundry.com/bronze-filament>, accessed 10/20/2019).
- [4] VirtualFoundry. (2019). *Material Safety Datasheet Bronze Filament* (<https://static1.squarespace.com/static/575b8367b09f95c081a40151/t/5aa7e857f9619a457039385c/1520953431491/TVF+MSDS+Bronze+Filamet%E2%84%A2+18+03-13.pdf>, accessed October 20, 2019).
- [5] ASTM, "ASTM D790 03 - Standard Test Methods for Flexural Properties of Unreinforced and Reinforced Plastics and Electrical Insulating Materials," ed.
- [6] (2019). *Phase Diagram of Copper (Cu) and Tin (Sn)* (https://www.tf.uni-kiel.de/matwis/amat/iss/kap_6/illustr/i6_2_1.html, accessed 10/22/2019).
- [7] A. R. Torrado Perez, D. A. Roberson, and R. B. Wicker, "Fracture Surface Analysis of 3D-Printed Tensile Specimens of Novel ABS-Based Materials," *Journal of Failure Analysis and Prevention*, vol. 14, pp. 343-353, 2014/06/01 2014.